

Impact of Nucleon Mass Shift on the Freeze Out Process

Sven Zschocke

Section for Theoretical and Computational Physics,

and Bergen Computational Physics Laboratory,

University of Bergen, 5007 Bergen, Norway and

Forschungszentrum Rossendorf, 01314 Dresden, Germany

László Pál Csébai

Section for Theoretical and Computational Physics,

and Bergen Computational Physics Laboratory,

University of Bergen, 5007 Bergen, Norway and

MTA-KFKI, Research Institute of Particle and Nuclear Physics, 1525 Budapest 114, Hungary

Etele Molnár and Ágnes Nyíri

Section for Theoretical and Computational Physics,

and Bergen Computational Physics Laboratory,

University of Bergen, 5007 Bergen, Norway

Jaakko Manninen

Section for Theoretical and Computational Physics,

and Bergen Computational Physics Laboratory,

University of Bergen, 5007 Bergen, Norway and

University of Oulu, Department of Physical Sciences, 90571 Oulu, Finland

The freeze out of a massive nucleon gas through a finite layer with time-like normal is studied. The impact of in-medium nucleon mass shift on the freeze out process is investigated. A considerable modification of the thermodynamical variables temperature, flow-velocity, energy density and particle density has been found. Due to the nucleon mass shift the freeze out particle distribution functions are changed noticeably in comparison with evaluations, which use vacuum nucleon mass.

PACS numbers:

I. INTRODUCTION

High-energy nucleus-nucleus collision experiments are mainly designed for the search and investigation of the predicted new state of matter, the Quark-Gluon Plasma (QGP), in which quarks and gluons would be set free from the color confinement observed in normal nuclear matter. Moreover, heavy-ion reactions are expected to exhibit other phenomena of Quantum Chromodynamics (QCD) in the hot and dense environment of the collision region, like in-medium modifications of almost all hadrons, or the state of Color Superconductivity (CSC). In this respect, the nucleus-nucleus collision experiments provide a unique way to test the validity of present theoretical approaches and models of physics of strongly interacting matter.

On the other side, a characteristic and inevitable problem of collision experiments is that in-medium modifications of hadrons and the expected new states of matter (e.g. QGP, CSC) disappear by the end of the reaction. Accordingly, one can not directly measure these properties of the produced hot and dense medium. Instead, one has to probe the initial stages of the collision indirectly by using theoretical models to reproduce the observed final particle spectra. A detailed understanding of

the different stages of a relativistic heavy-ion collision process becomes therefore very compelling. The scheme of a representative relativistic heavy-ion collision process looks as follows:

In the very early stage of nucleus-nucleus collisions, an extremely hot and dense medium is created in which several hundred or even thousands of secondary partons are produced. Due to the high partonic density, local (perhaps global) thermal equilibrium is reached very rapidly, for instance, at RHIC or LHC incident energies within $(0.3 - 0.5)$ fm/c for gluons, and $(0.5 - 1.0)$ fm/c for quarks [1, 2, 3, 4]. It has been proposed that since the heavy quark flavor production is dominated by the relatively slow gluon-gluon fusion, chemical equilibration of the heavy quark flavors (strangeness, charm etc.) might stay incomplete during all the collision evolution, so that there is a need to implement a strangeness suppression factor γ_s [5]. Nevertheless, chemical equilibration of gluons and light quark flavors is believed to be reached around 2 fm/c [6].

In spite of the nature of the produced medium, large pressure gradient perpendicular to the collision axes drives the system into rapid expansion and to cool down. In heavy-ion collisions, below the critical temperature $T_c \simeq 175$ MeV several

hundred of hadrons emerge forming a strongly interacting resonance gas. As the fireball cools down further, below the chemical freeze out temperature T_{ch} , inelastic collisions cease and hadronic abundances become fixed. This process is usually called the chemical freeze out (cFO). Later on, when the hadron gas becomes more dilute, below the thermal freeze out temperature T_{th} , the elastic interactions cease as well. This stage of the collision is usually called kinetic freeze out (kFO). Finally, the formed hadrons of the thermal freeze out spectrum propagate freely toward the detectors. Recently, in [7] both the chemical freeze out temperature T_{ch} and thermal freeze out temperature T_{th} have been determined for several collision scenarios and baryon densities. Nonetheless, the sharp distinction between chemical and thermal freeze out is an idealization, while in a real collision due to the short time scales both processes become mixed with each other. Therefore, one sometimes calls it freeze out process without further specification between chemical and thermal freeze out which implies $T_{ch} \simeq T_{th}$.

Many kind of approaches have been applied for the description of the freeze out of strongly interacting matter. Statistical models [7, 8, 9, 10, 11, 12, 13, 14] can reproduce well the measured particle multiplicities in most of the collision experiments done so far. Kinetic models [15, 16] as well as hydrodynamical approaches [17] have proven to be able to describe most of the collective phenomena like the different flow components in heavy-ion reactions. However, despite the success in comparison with experiments, the in-medium modifications of the hadrons during the freeze out process have not been taken into account yet. In most of the former evaluations the vacuum parameters of the particles have been implemented. To the best of our knowledge the Refs. [18, 19] seem to be the only investigations, where the impact of in-medium hadron masses (mesons and baryons) on the particle ratios during the chemical freeze out has been studied. A systematic study about the impact of in-medium hadron masses on the kinetic freeze out process has not been performed yet.

But, implementing the vacuum parameters of hadrons for describing the kinetic freeze out process is an approximation which may work or may not work, depending on the physical system under consideration. For instance, both experiments [20] and theoretical investigations [21, 22, 23] suggest, that pions embedded in a hot and dense medium suffer only a small mass change. Accordingly, the description of the freeze out process of a purely pion gas by means of their vacuum parameters seems to be a reliable approximation. On the other side, the mass of kaons can be shifted considerably in a hot and dense medium [24, 25, 26], so that taking into account in-medium modifications for

the kaon component seems to be compelling.

In this work, we study a nucleon gas and investigate how strong the impact of an in-medium mass shift of nucleons on the freeze out profile is. We compare the obtained results with calculations using a vacuum nucleon mass.

The paper is organized as follows: The freeze out process within a finite time-like layer is considered in Sec. 2. The nucleon mass shift and it's implementation into the freeze out process are outlined in Sec. 3. The results of our study are presented in Sec. 4. Finally, in Sec. 5 a summary and outlook are given. Further notations and a brief mathematical remark can be found in the Appendix.

II. FREEZE OUT PROCESS WITHIN A FINITE LAYER

In this section we are focussing on the last stage of the collision, the freeze out process, i.e. we start our investigation from the time of collision where the expanding and cooling down system reaches a temperature $T \leq T_c$, where the hadronization of the primary parton gas is almost completed.

The frozen out particles are formed in a layer of finite thickness L , bounded by two hyper-surfaces: the pre-freeze out hyper-surface with $T_{\text{pre FO}} \simeq T_c$ and a post-freeze out hyper-surface with $T_{\text{post FO}} \simeq T_{ch} \simeq T_{th}$. These surfaces are defined by the normal $d\sigma_\mu$, which in general can be a space-like $d\sigma_\mu d\sigma^\mu < 0$ or time-like four vector, $d\sigma_\mu d\sigma^\mu > 0$. The diameter L of the layer is of the order of a few mean free paths of the particle under consideration. To get an idea about the scales we recall that for nucleons at ground state saturation density the mean free path is about 1 fm [27, 28].

Dynamical models, like hydrodynamical or transport models, allow to describe such freeze out processes through the layer. In doing so, the hydrodynamical models have certain advantages over transport model calculations. An important one is that, once the equation of state and initial conditions of the hadronic matter are specified, the space-time evolution of the system is uniquely determined by the hydrodynamic differential equations. Especially, this implies that the impact of several equation of state may be investigated in a very direct way. Even more, uncertainties or assumptions made in the underlying kinetic theory of the particles under consideration are circumvented. In addition, the use of familiar thermodynamical concepts, like temperature, flow velocity, pressure and energy density also provide a transparent physical picture of the evolution. Of course, the basis of applicability of hydrodynamics is the assumption of local thermal and chemical equilibrium. In the following we will suppose the validity of these conditions and will apply the theory of hy-

drodynamics for describing the thermal freeze out process in a finite space-time layer.

The theoretical description of the kinetic freeze out within a hydrodynamical approach has been worked out some years ago [29, 30, 31, 32, 33]. Very recently, in [34] and [35] the formalism has been applied to the case of a finite freeze out layer, separately both for space-like and time-like normals. While the formalism in [34, 35] has been developed for the general case of a massive particle, the calculations have been performed for a massless pion gas. Here, we will make use of the outlined formalism of Ref. [35] for a time-like layer for the case of a massive nucleon. In particular, we will implement the in-medium mass modification of nucleons traveling through the freeze out layer. It is not necessary to repeat the formalism of [35] in detail. Instead, we shall restrict our explanations on the basic concept and will only give the equations relevant for our study.

Local equilibrium implies that the thermodynamical parameters inside the layer become space-time dependent, i.e. we have a space-time dependent temperature $T(x)$, flow velocity $v(x)$, energy density $e(x)$ and nucleon density $n(x)$. For evaluating these functions we need the basic equations of hydrodynamics,

$$\partial_\mu N^\mu(x) = 0, \quad \text{and} \quad \partial_\mu T^{\mu\nu}(x) = 0, \quad (1)$$

where

$$N^\mu(x) = \int \frac{d^3\mathbf{k}}{k^0} k^\mu f(x, k) \quad (2)$$

is the particle current, and

$$T^{\mu\nu}(x) = \int \frac{d^3\mathbf{k}}{k^0} k^\mu k^\nu f(x, k) \quad (3)$$

is the energy momentum tensor. Here, $x^\mu = (t, \mathbf{r})$ is the four-coordinate and $k^\mu = (E_k, \mathbf{k})$ is the four-momentum of the nucleon. While the first relation in (1) is only valid when the total number of particles is conserved, the second relation in (1) is always satisfied and asserts the energy and momentum conservation. The one-particle distribution function $f(x, k)$ is an invariant Lorentz scalar, and is normalized to the invariant number of particles N (in our case the nucleons), i.e. $N = \int d^3\mathbf{r} d^3\mathbf{k} f(x, k)$.

While the components of the tensors (2) and (3) depend on the Lorentz frame chosen, two Lorentz invariant scalars can be obtained, the invariant scalar energy density e and invariant scalar particle density n :

$$e(x) = u_\mu(x) T^{\mu\nu}(x) u_\nu(x), \quad (4)$$

$$n(x) = u_\mu(x) N^\mu(x). \quad (5)$$

We notice that these invariant scalars have to be distinguished from the non-invariant energy density $\tilde{e} = E/V$ and particle density $\tilde{n} = N/V$, where E is the non-invariant total energy and V is the non-invariant volume of the system.

While the invariant relations (4) and (5) are valid in any Lorentz frame, in a concrete evaluation one has to specify the frame in which the components of the four-current, energy-momentum tensor and the (always time-like) four-velocity u_μ are evaluated. Any Lorentz frame can be defined by a Lorentz boost in respect to the local Rest Frame of the nucleon Gas, RFG, on which the condition $u_{\text{RFG}}^\mu(x) = (1, 0, 0, 0)$ is imposed; obviously, in RFG we have $\tilde{e} = e_{\text{RFG}}$ and $\tilde{n} = n_{\text{RFG}}$. However, this condition does not define the RFG uniquely. There are, in general, several possibilities to define such a rest frame. Here, we will take Eckart's definition [36], which is the most appropriate one for heavy-ion reactions with high baryon densities. According to this definition the local Rest Frame is tied to conserved particles, which can be achieved by equating the unit vector of the particle four-current with the four-velocity of the particle flow,

$$u^\mu(x) = \frac{N^\mu(x)}{\sqrt{N^\nu(x)N_\nu(x)}}. \quad (6)$$

Accordingly, in RFG there is no particle flow in spatial directions. It is straightforward to recognize, that the Lorentz invariant denominator in (6) is just the invariant scalar particle density of Eq. (5). And, while the components of four-vectors u^μ and N^μ depend on the Lorentz frame chosen, the tensor relation (6), which connects these frame-dependent components, remains valid in any frame.

From the definitions (4), (5) and (6) one obtains the following set of three coupled differential equations, which, by means of Eckart's definition, are valid in any Lorentz frame:

$$\begin{aligned} de(x) &= u_\mu(x) dT^{\mu\nu}(x) u_\nu(x) \\ &\quad + 2 du_\mu(x) T^{\mu\nu}(x) u_\nu, \end{aligned} \quad (7)$$

$$dn(x) = u_\mu(x) dN^\mu(x), \quad (8)$$

$$du^\mu(x) = \frac{1}{n(x)} \left(g^{\mu\nu} - u^\mu(x) u^\nu(x) \right) dN_\nu. \quad (9)$$

Altogether, since there are four unknowns in the problem under consideration, namely T, v, e, n , an additional constraint is necessary to get a complete system of equations, which uniquely determines these four unknowns. That constraint is provided by the Equation of State (EoS) for the nucleon gas [37, 38, 39], which is assumed to be valid in any space-time point of the reaction zone

after hadronization,

$$e(x) = n(x) \left[M_N(n(x), T(x)) - E_0 + \frac{K}{18} \left(\frac{n(x)}{n_0} - 1 \right)^2 + \frac{3}{2} T(x) \right]. \quad (10)$$

The term $E_0 = 16$ MeV accounts for the nuclear binding energy among the nucleons, the term proportional to the compressibility constant $K = 9(\partial p/\partial n)_{n=n_0} \simeq 235$ MeV accounts for the dependence of compressibility on density. Since we are aiming at investigating the impact of in-medium nucleon mass shift on the freeze out process, we have already implemented a density and temperature dependent nucleon pole mass in (10). The given EoS (10) is a generalization of EoS for the ideal nucleon gas, which is valid in the rest frame, i.e. $e_{\text{RFG}} = n_{\text{RFG}}[M_N + 3/2 T_{\text{RFG}}]$. There are other generalizations for the nucleonic EoS [36]. However, we have checked that in the energy and temperature region we are working here, the results obtained are insensitive on the specific choice of nucleonic EoS. The EoS (10) is used to determine the temperature $T(x)$ of the interacting component of the nucleon gas during the freeze out process. Accordingly, the four equations (7), (8), (9) and (10) represent a closed set for evaluating the four unknowns T, v, e, n of the one-particle system.

Now we will turn to the explicit evaluation of components for the energy-momentum tensor and nucleon four-current. In line with Ref. [35] we will perform all evaluations in the Lorentz Rest Frame of the freeze out Front, RFF, so that in our study all tensor components in Eqs. (7) - (9) can be labeled by RFF. The Lorentz frame RFF is defined as follows:

At a given instant in the space-time the expanding hot and dense hadronic system reaches a certain freeze out temperature $T_{\text{post FO}}$, where all constituents of the system are assumed to get frozen out, i.e. all hadrons do not interact anymore. In an arbitrary but fixed direction $\mathbf{e}_x = \mathbf{r}_T/|\mathbf{r}_T|$ transverse to the beam the Rest Frame of the gas RFG moves with a velocity \mathbf{v}_T relative to the freeze out front RFF. Then, by means of a Lorentz transformation the particle four-velocity in RFF becomes $u_{\text{RFF}}^\mu = \gamma(1, v, 0, 0)$ where $v = \text{sign}(\mathbf{v}_T)|\mathbf{v}_T|$ and $\gamma = 1/\sqrt{1-v^2}$. The velocity v is called flow-velocity and, in general, can be positive, negative or even zero.

Furthermore, as the system expands and cools down the number of interacting particles decreases up to the post freeze out surface of the finite layer, where by definition the density of interacting particles vanishes. Accordingly, the thermal freeze out process inside the layer can be described by decomposing the particle distribution function into two components of the matter, an interacting part f_i

and a non-interacting free part f_f , thus

$$f(x, k) = f_i(x, k) + f_f(x, k). \quad (11)$$

According to Eq. (11) and by means of (2), (5), (6) we have an interacting and a non-interacting particle density,

$$n_i(x) = \sqrt{N_{\nu i}(x) N_i^\nu(x)}, \\ n_f(x) = \sqrt{N_{\nu f}(x) N_f^\nu(x)}, \quad (12)$$

with $n = n_f + n_i$. On the pre-freeze out we assume to have thermal equilibrium, i.e. we have a Jüttner distribution for f_i as starting one-particle distribution function, while by definition f_f is zero on the pre-freeze out hyper-surface. The space-time evolution of the interacting and non-interacting components inside the layer is governed by the following differential equations [35]:

$$\partial_t f_i = -\frac{1}{\tau} \left(\frac{L}{L-t} \right) \left(\frac{k^\mu d\sigma_\mu}{k_\mu u^\mu} \right) f_i + \frac{1}{\tau_0} [f_{eq}(t) - f_i], \quad (13)$$

$$\partial_t f_f = +\frac{1}{\tau} \left(\frac{L}{L-t} \right) \left(\frac{k^\mu d\sigma_\mu}{k_\mu u^\mu} \right) f_i, \quad (14)$$

with the time τ between collisions. The Jüttner distribution is given as [40]

$$f_{eq}(t) = \frac{1}{(2\pi\hbar)^3} e^{(\mu - k^\mu u_\mu)/T}, \quad (15)$$

with the chemical potential μ ; for the interacting component it is determined by Eq. (33) given below. The second term in (13) is the re-thermalization term [29, 30, 32, 33, 35] which describes how fast the interacting component approaches the Jüttner distribution within a relaxation time τ_0 . Here, we will use the immediate re-thermalization limit $\tau_0 \rightarrow 0$, which implies $f_i \rightarrow f_{eq}$ faster than $\tau_0 \rightarrow 0$, i.e. local equilibrium at all times during the freeze out in the following way:

First, the layer is subdivided into small intervals. Then we calculate the changes $dT^{\mu\nu}$ and dN^μ based on their kinetic definitions (2) and (3), respectively, with the freeze out distribution f_i . At the beginning of a time step this is considered to be a flux coming from a Jüttner distribution, and continues during the length of the whole time step according to the kinetic differential equation (13) (without the re-thermalization term). Then the remaining distribution is not of Jüttner type anymore. Nevertheless, the loss dT and dN are calculated based on the initial Jüttner and the escape probability. When we are at the end of the time step of such a small interval of the layer, we

have a change in all thermodynamical variables T, v, e, n . With $\tau_0 \rightarrow 0$ we assume an immediate re-thermalization of $T^{\mu\nu}$ and N^μ , i.e. we define a new Jüttner distribution with the new values for T, v, n at the end of the time step. At the next time step we use this new Jüttner distribution to calculate the changes of it in the next small time interval, and so on. Accordingly, the last term in (7) vanishes, as it can be seen as follows. Since at the beginning of a time step we take a Jüttner distribution according to the immediate re-thermalization limit, the second term of (7) is zero (see Appendix). Then, during a time step the energy momentum tensor (3) of a Jüttner distribution is changed by an amount of $dT^{\mu\nu} \sim dt$, governed by Eq. (13). That means the second term in (7) is of order $\mathcal{O}(du dt)$, i.e. of second order in the differentials, so that the second term in (7) has to be neglected. For more details about the relations (13) and (14) and about the re-thermalization limit we refer the interested reader to Refs. [29, 30, 33, 35].

By means of the microscopic definitions (2) and (3) one obtains for the change of the four-current and energy momentum tensor the following general expressions for the interacting component ,

$$dN_i^\mu = dt \int \frac{d^3 \mathbf{k}}{k^0} k^\mu \left[\partial_t f_i \right], \quad (16)$$

$$dT_i^{\mu\nu} = dt \int \frac{d^3 \mathbf{k}}{k^0} k^\mu k^\nu \left[\partial_t f_i \right]. \quad (17)$$

Since we are mainly interested on the freeze out of the interacting nucleons we will write down the interacting component of these tensors and drop the index i in the following. The non-interacting components can be deduced from them by changing the sign in front. We will write down these expressions explicitly for the change of dN and dT as given in Ref.[35] for the RFF, which, as previously mentioned, are related to the RFG by a Lorentz boost:

$$\frac{dN^0(t, v, T, M_N, n)}{dt} = \frac{1}{\tau} \frac{L}{L-t} \frac{n}{4} (G_1^-(M_N, v, T) - G_1^+(M_N, v, T)), \quad (18)$$

$$\frac{dN^x(t, v, T, M_N, n)}{dt} = \frac{1}{v} \frac{dN^0(t, v, T, M_N, n)}{dt} + \frac{1}{\tau} \frac{L}{L-t} \frac{n}{4} \left(\frac{4aK_1(a)}{v} + \frac{2a^2K_0(a)}{v} \right), \quad (19)$$

$$\frac{dT^{00}(t, v, T, M_N, n)}{dt} = \frac{1}{\tau} \frac{L}{L-t} \frac{nT}{4} \frac{1}{\gamma v} (G_2^-(M_N, v, T) - G_2^+(M_N, v, T)), \quad (20)$$

$$\begin{aligned} \frac{dT^{0x}(t, v, T, M_N, n)}{dt} = & \frac{1}{v} \frac{dT^{00}(t, v, T, M_N, n)}{dt} \\ & + \frac{1}{\tau} \frac{L}{L-t} \frac{nT}{2} \frac{b^2}{v} ((3+v^2)K_2(a) + aK_1(a)), \end{aligned} \quad (21)$$

$$\begin{aligned} \frac{dT^{xx}(t, v, T, M_N, n)}{dt} = & \frac{1}{v} \frac{dT^{0x}(t, v, T, M_N, n)}{dt} \\ & - \frac{T}{\gamma v} \left(\frac{dN^x(t, v, T, M_N, n)}{dt} - \frac{1}{v} \frac{dN^0(t, v, T, M_N, n)}{dt} \right) \\ & + \frac{1}{\tau} \frac{L}{L-t} \frac{nT}{2} ab \left(\frac{1}{v^2} (1+3v^2)K_2(a) + bK_1(a) \right). \end{aligned} \quad (22)$$

Here, $a = M_N/T$ and $b = \gamma a$. The functions G_n^\pm and K_n are defined in the Appendix. The set of equations (7) - (10) and (18) - (22) allow us to evaluate the basic thermodynamical function $T(x), v(x), e(x)$ and $n(x)$ during the freeze out process for a particle with a constant mass M_N . However, as mentioned in the Introduction we are aiming at an implementation of in-medium mass shift to look for it's impact on the freeze out process.

Therefore, we will first evaluate the equation with the vacuum nucleon pole mass $M_N(0)$, and afterwards replace it by a density and temperature dependent nucleon pole mass $M_N(n, T)$.

III. NUCLEON MASS SHIFT

During the freeze out process, the temperature and particle densities are presumably close to the deconfinement phase transition critical values [7]. Therefore, the in-medium values of masses, decay widths, coupling constants, and all other physical quantities characterizing the particles under consideration have to be taken into account. In our study we examine a purely nucleon gas, and consider the in-medium mass modification of nucleons located in a hot and dense nuclear environment.

We start with a brief reconsideration of the nucleon mass in vacuum. The nucleon derives its vacuum mass, $M_N(0) = 939$ MeV, from the quark-gluon interaction of its underlying substructure, consisting of valence quarks, sea quarks and gluons. However, although there has been considerable success in reproducing the vacuum mass of nucleons on the basis of their microscopic quark and gluon substructure (lattice evaluations, [41]), a rigorous use of fundamental theory of QCD in this respect is not yet in reach. Therefore, our understanding of the nucleon's mass structure comes mostly from models. From a hadronic field theoretical point of view the nucleon mass $M_N(0)$ can be defined as the pole mass of the nucleon propagator in vacuum,

$$\Pi_N(k) = i \int d^4x e^{ikx} \langle 0 | T \hat{\Psi}_N(x) \hat{\bar{\Psi}}_N(0) | 0 \rangle = \frac{1}{\gamma_\mu k^\mu - \overset{\circ}{M}_N - \Sigma_N(k) + i\epsilon}, \quad (23)$$

where T is the Dirac time-ordering, $\hat{\Psi}_N$ is the nucleon field operator, $\hat{\bar{\Psi}}_N = \hat{\Psi}_N^\dagger \gamma_0$, γ_μ are the Dirac matrices, and $\Sigma_N(k)$ is the nucleon self energy in vacuum. The parameter $\overset{\circ}{M}_N$ is called bare nucleon mass, i.e. the mass parameter entering the Lagrangian which describes the interaction between the nucleons and other hadrons (e.g. nucleon-pion interaction). In general, the mass parameter $\overset{\circ}{M}_N$ has to be distinguished from the vacuum pole mass of nucleon $M_N(0) = 939$ MeV, defined by

$$M_N(0) = \overset{\circ}{M}_N + \text{Re}\Sigma_N(\gamma_\mu k^\mu = M_N(0)). \quad (24)$$

As mentioned, there are several models which allow to calculate the pole mass from a QCD based microscopic point of view. Among them is the extension of QCD sum rule approach [42] to the case of baryons [43], which provides an interlocking between the nucleon pole mass and QCD based quantities, so called QCD condensates. Within the QCD sum rule approach, the nucleon field operator $\hat{\Psi}_N$ in (23) is expressed by an interpolating field $\hat{\eta}_N$ [43], which is made of up and down quark field operators, and which has the quantum numbers of a nucleon (charge, spin, isospin, parity). In

this line, in [43] the so called Ioffe formula for the nucleon pole mass in vacuum has been obtained,

$$M_N(0) = -\frac{8\pi^2}{M^2} \langle 0 | \bar{q}q | 0 \rangle, \quad (25)$$

providing a link between the pole mass and the chiral condensate, $\langle 0 | \bar{q}q | 0 \rangle = -(0.250 \text{ GeV})^3$; $M \simeq 1.15 \text{ GeV}$ is the Borel mass parameter determined by stability constraint of the nucleon sum rule approach [43].

Now we will turn to the in-medium nucleon pole mass $M_N(n, T)$, which is the very characteristics which enters the EoS (10), [44]. In general, a nucleon propagating in a hot and dense hadronic environment can be regarded as a quasi particle, described by the in-medium nucleon correlator

$$\begin{aligned} & \Pi_N(k, n, T) \\ &= i \int d^4x e^{ikx} \langle \Omega | T \hat{\Psi}_N(x) \hat{\bar{\Psi}}_N(0) | \Omega \rangle, \\ &= \frac{1}{\gamma_\mu k^\mu - \overset{\circ}{M}_N - \Sigma_N(k, n, T) + i\epsilon}. \end{aligned} \quad (26)$$

The nucleon self energy $\Sigma_N(k, n, T)$ in medium depends on density and temperature of the surrounding hadronic medium inside the freeze out layer; the hadronic medium is described by the state $|\Omega\rangle$. In generalization of Eq. (24) the in-medium nucleon pole mass is defined by

$$\begin{aligned} & M_N(n, T) \\ &= \overset{\circ}{M}_N + \text{Re}\Sigma_N(\gamma_\mu k^\mu = M_N(n, T), n, T). \end{aligned} \quad (27)$$

From this point of view it becomes obvious that the pole mass will be modified in a hot and dense hadronic matter, simply due to the fact that the self energy of a nucleon in medium will be different from a nucleon in vacuum.

In general, the particle pole mass in (27) for a nucleon at rest (RFG), embedded in a hot and dense hadronic medium, is given by [45, 46]

$$\begin{aligned} & M_N(n, T) \\ &= M_N(0) + \text{Re}\Sigma_S(n, T) + \text{Re}\Sigma_V(n, T), \end{aligned} \quad (28)$$

with the attractive scalar part ($\text{Re}\Sigma_S < 0$) and the repulsive vector part ($\text{Re}\Sigma_V > 0$) of nucleon self energy in medium. It is a result of several theoretical models applied so far, that the individual contributions of scalar and vector self energy are large, but they are canceled by each other to a large extent; typical values at saturation density are $\text{Re}\Sigma_S = -400$ MeV, $\text{Re}\Sigma_V = +300$ MeV [45, 46, 47]. In particular, several theoretical approaches predict a mass dropping of the nucleon pole mass in a hadronic environment of about

$M_N(n_0, 0) - M_N(0) \simeq -(80 \pm 20)$ MeV at ground-state nuclear saturation density $n_0 = 0.17 \text{ fm}^{-3}$ and at vanishing temperature. Here, we will take the QCD sum rule results for a nucleon in matter, given by [45, 46]

$$\text{Re}\Sigma_S(n, T) = +M_N(0) \left(\frac{\langle \Omega | \bar{q}q | \Omega \rangle}{\langle 0 | \bar{q}q | 0 \rangle} - 1 \right), \quad (29)$$

$$\text{Re}\Sigma_V(n, T) = -\frac{8}{3}M_N(0) \frac{\langle \Omega | q^\dagger q | \Omega \rangle}{\langle 0 | \bar{q}q | 0 \rangle}, \quad (30)$$

where we have accounted for the lowest mass dimension condensates only; gluon condensate and higher mass dimension condensates give only small corrections due to large cancellations between their individual contributions. We recall that the part $M_N^* \equiv M_N(0) + \text{Re}\Sigma_S$ of (28) resembles the terminology "effective mass" used in the Walecka model [48], the Skyrme model [49], and which has also been evaluated by means of a mean field approach in [50]. For a more detailed clarifying of the terminology "effective mass", often used in different meaning, we refer to Ref. [51], where M_N^* is called Dirac mass.

The chiral condensate at finite temperature and density, $\langle \Omega | \bar{q}q | \Omega \rangle$, has been evaluated within the Nambu-Jona-Lasinio (NJL) model in Ref. [52]. Later, in Ref. [53] the in-medium chiral condensate has been evaluated at finite densities and temperatures by means of a pion-nucleon gas, finding a good agreement with the results of Ref. [52]. Here, the condensates (29) and (30) have to be evaluated for a purely nucleon gas to be consistent within the whole approach presented. According to Eqs. (11) and (12) there are two components inside the finite layer: an interacting component with density n_i and a non-interacting component with density n_f . For evaluating the condensates (29) and (30) we approximate the interacting component by a Fermi gas with chemical potential μ_i and temperature T . On the other side, the temperature for the non-interacting component becomes ill-defined. Nonetheless, a relevant physical parameter for describing the non-interacting component remains the density n_f . Accordingly, the condensates in one-particle approximation are given as follows [53]:

$$\begin{aligned} \langle \Omega | \bar{q}q | \Omega \rangle &= \langle 0 | \bar{q}q | 0 \rangle \\ &+ 4 \int \frac{d^3 \mathbf{k}}{(2\pi)^3} \frac{1}{2E_k} N_F \langle N(\mathbf{k}) | \bar{q}q | N(\mathbf{k}) \rangle \\ &+ \frac{n_f}{2M_N(0)} \langle N(\mathbf{k}) | \bar{q}q | N(\mathbf{k}) \rangle, \end{aligned} \quad (31)$$

$$\begin{aligned} \langle \Omega | q^\dagger q | \Omega \rangle &= 4 \int \frac{d^3 \mathbf{k}}{(2\pi)^3} \frac{1}{2E_k} N_F \langle N(\mathbf{k}) | q^\dagger q | N(\mathbf{k}) \rangle \\ &+ \frac{n_f}{2M_N(0)} \langle N(\mathbf{k}) | q^\dagger q | N(\mathbf{k}) \rangle. \end{aligned} \quad (32)$$

where $N_F = [e^{(E_k - \mu_i)/T} + 1]^{-1}$ is the Fermi distribution, and the nucleon energy is $E_k = \sqrt{M_N(0)^2 + \mathbf{k}^2}$. Note that $\langle 0 | q^\dagger q | 0 \rangle = 0$. Here, the relativistic normalization $\langle N(\mathbf{k}_1) | N(\mathbf{k}_2) \rangle = 2E_{k_1}(2\pi)^3 \delta^{(3)}(\mathbf{k}_1 - \mathbf{k}_2)$ is used. In Eqs. (31) and (32) the spin (up, down) and isospin (proton, neutron) degeneracy of nucleon states has been taken into account by the factor 4 in front of the momentum integrals. The chemical potential for the interacting component can be evaluated via

$$n_i = 4 \int \frac{d^3 \mathbf{k}}{(2\pi)^3} \frac{1}{e^{(E_k - \mu_i)/T} + 1}. \quad (33)$$

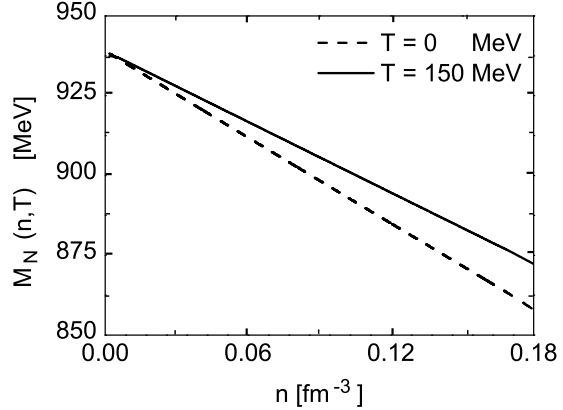


FIG. 1: Effective in-medium nucleon pole mass $M_N(n, T)$ according to Eq. (28) (for more details see main text).

The condensates in Fermi gas approximation are given by [54]

$$\langle N(\mathbf{k}) | \bar{q}q | N(\mathbf{k}) \rangle = \frac{M_N(0)\sigma_N}{m_q}, \quad (34)$$

$$\langle N(\mathbf{k}) | q^\dagger q | N(\mathbf{k}) \rangle = 3M_N(0). \quad (35)$$

The nucleon sigma term is $\sigma_N \simeq 50$ MeV [55], and $m_q \simeq 5$ MeV is the averaged current quark mass of the up and down quark flavor [56, 57]. Inserting these parameters into (29) and (30) we obtain $\text{Re}\Sigma_S = -390$ MeV and $\text{Re}\Sigma_V = +315$ MeV at ground state saturation density n_0 . The Eqs. (28) - (35) summarize our propositions made for obtaining the in-medium nucleon pole mass $M_N(n, T)$ which enters the EoS (10). Fig. (1) shows the dropping of the in-medium nucleon pole mass. The slight increase of the in-medium nucleon pole mass with temperature is an artifact of the purely nucleon gas approximation. That means, an implementation of pions in Eqs. (31) and (32) which govern the mass relation (28), would cause a temperature decreasing of these condensates [53] and

then of the in-medium nucleon pole mass. Here, in a baryon dominated system this artificial increase of $M_N(n, T)$ with temperature is superposed by the much stronger down shift of the pole mass with nucleon density.

IV. RESULTS AND DISCUSSION

In this section we represent and discuss the results of the coupled set of differential equations (7) - (9) in combination with the EoS (10) and the in-medium nucleon mass shift relations (28) - (35). The differential equations have been solved with the Runge-Kutta method [58, 59, 60] on the IBM 1300 cluster at Bergen Center for Computational Science (BCCS). For all of the calculations, we have taken $T_{\text{pre FO}} = 150$ MeV, $n_{\text{pre FO}} = 1.5 n_0$ (corresponding to $\mu_{\text{pre FO}} \simeq 615$ MeV) and $v_{\text{pre FO}} = 0.5 c$ as starting values on the pre freeze out hypersurface. These values are, for instance, in line with typical parameters which have been reached within the Alternating-Gradient Synchrotron (AGS) at *Brookhaven National Laboratory* (BNL) in Brookhaven/USA, cf. [61]. Higher baryonic densities can be reached within the Schwer-Ionen-Synchrotron (SIS) at *Gesellschaft für Schwerionenforschung* (GSI) in Darmstadt/Germany, cf. [62]. Note that $T_{\text{pre FO}}$ and $n_{\text{pre FO}}$ are pre freeze out values and, therefore, they are larger than typical post freeze out values given, for instance, in Ref. [7].

In Figs. 2 and 3, the time evolution of the primary thermodynamical functions through the finite freeze out layer are shown, in terms of the proper time τ . Note that the densities $n = n_i + n_f$ and $e = e_i + e_f$ are kept constant inside the layer.

We find a substantial impact of in-medium mass modification on the freeze out process within the purely nucleon gas model. Furthermore, the Figs. 2 and 3 also elucidate, that the freeze out process proceeds faster for all thermodynamical quantities T, v, e, n when taking into account the mass dropping of nucleons. The physical reason for a faster freeze out originates from a smaller energy density of the nucleon system due to a smaller nucleon mass $M_N(n, T)$ compared to the vacuum nucleon mass $M_N(0)$.

The given functions for T, v, e, n are not directly accessible. In experiments the way to study the hot and dense hadronic matter produced in heavy-ion collisions is to measure the distributions of final state particles, which reach the detectors long time

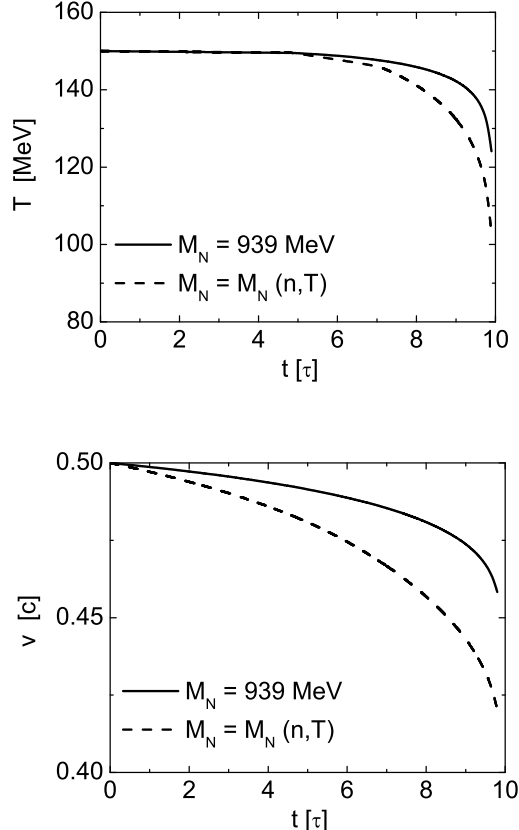


FIG. 2: **LEFT:** The temperature of the interacting component. **RIGHT:** The flow velocity parameter v of the interacting component. The solid lines are with a constant nucleon mass $M_N(0) = 939$ MeV, while the dashed curves are evaluated with a density and temperature dependent nucleon mass $M_N(n, T)$.

after their last interaction. Accordingly, as next we consider the one-particle freeze out distribution function at $k_y = 0$, i.e. $f_f(k_x) \equiv f_f(k_x, k_y = 0)$ and consider the impact of the evaluated thermodynamical functions T, v, e, n on it. The results are shown in Fig. 4 for different instants during the freeze out process. The function $f_f(k_x)$ is determined at the point A [63] of the freeze out front; see also Ref. [35] for more details. The function $f_f(k_x)$ is obtained by solving the differential equation (14), where for f_i the Jüttner distribution (15) is used, but with the parameters T and v as determined previously and given in Fig. 2.

The logarithmic scale in Fig. 4 disguised the strong modification of these distribution functions. For small moments up to $k_x \leq 1$ GeV, at the very beginning of the freeze out process at $t = 0.1 \tau$ there is a change of $f_f(k_x)$, which remains up to the end of the freeze out process at $t = 9.0 \tau$. A contour plot of the freeze out particle distribution functions $f_f(k_x, k_y)$ over their transversal and lon-

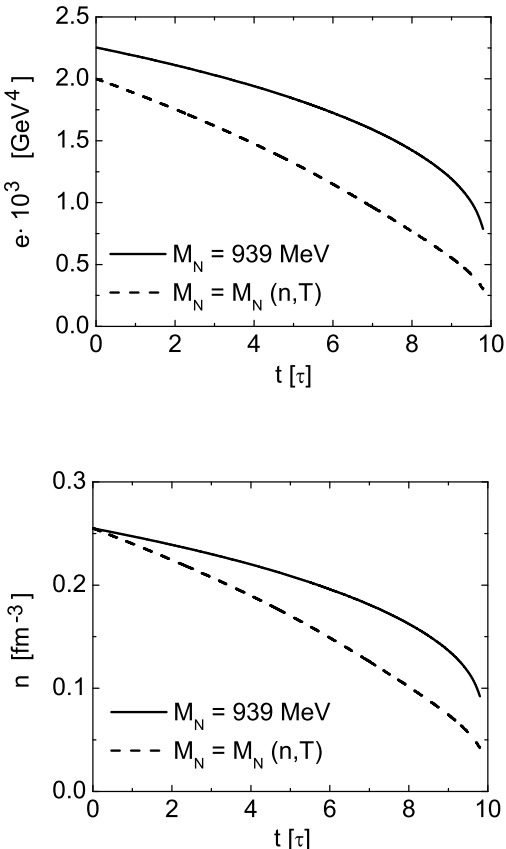


FIG. 3: **LEFT**: Nucleon energy density of the interacting component. **RIGHT**: Nucleon particle density of the interacting component. The solid lines are with a constant nucleon mass $M_N(0) = 939$ MeV, while the dashed curves are evaluated with a density and temperature dependent nucleon mass $M_N(n, T)$.

itudinal momenta k_x and k_y , respectively, shown in Fig. 5, illustrates this statement. We observe a remarkable change by a factor $\simeq 2$ for momenta $k_x, k_y \leq 1$ GeV.

A few remarks are in order about the used starting values for density and temperature. First, the formulas (29) and (30) have, like other theoretical approaches, a limited range of validity in respect to the density; $n \leq 1.5 n_0$. And second, according to Eq. (13) the re-thermalization is assumed within a time step dt . Numerical accuracy for solving the set of differential equations (7) - (9) requires sufficiently small time intervals dt . However, a smaller starting temperature $T_{\text{pre FO}}$ implies a longer re-thermalization time $\tau_0 < dt$, so that $T_{\text{pre FO}}$ cannot be taken arbitrary small. In addition, these two boundaries have to be adjusted to be in a region of the QCD phase diagram where we are inside the hadronization region and above the kinetic freeze out. The parameter choice of the starting values,

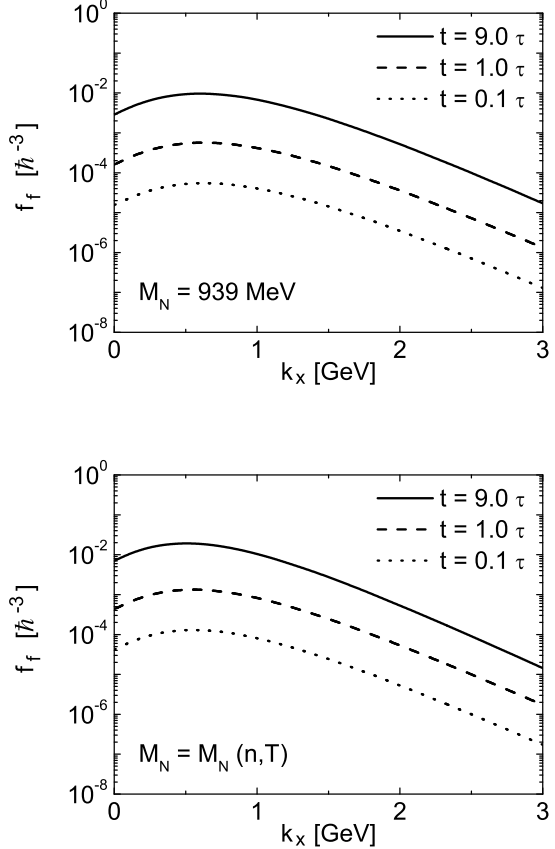


FIG. 4: **LEFT**: Freeze out distribution function $f_f(k_x, k_y = 0)$ at different instants t , evaluated with a constant nucleon mass $M_N(0) = 939$ MeV. **RIGHT**: Freeze out distribution function $f_f(k_x, k_y = 0)$ at different instants t , evaluated with the density and temperature dependent nucleon mass $M_N(n, T)$. The lines are as in the left panel. The Freeze out distribution function has increased by a factor of $\simeq 2$, when density and temperature dependent nucleon masses were taken into account.

$n_{\text{pre FO}} = 1.5 n_0$, $T_{\text{pre FO}} = 150$ MeV, are an optimal compromise for these borderlines. Within the approach presented we have a common way to model the kinetic freeze out process, and which is capable to implement the nucleon mass shift by means of a purely nucleon gas model. Nevertheless, one has also to be aware that the pion-nucleon ratio becomes small only for high enough nucleon densities $n = (1.5 - 2)n_0$ and moderate temperatures $T \simeq 100$ MeV, e.g. [8]. Our starting values for density and temperature on the pre freeze out hypersurface deviate from these values. Therefore, a more sophisticated model requires the implementation of pions and maybe even heavier mesons. However, due to different freeze out scenarios between nucleons and mesons, cf. [64], such a procedure would require the use of a two-fluid or even

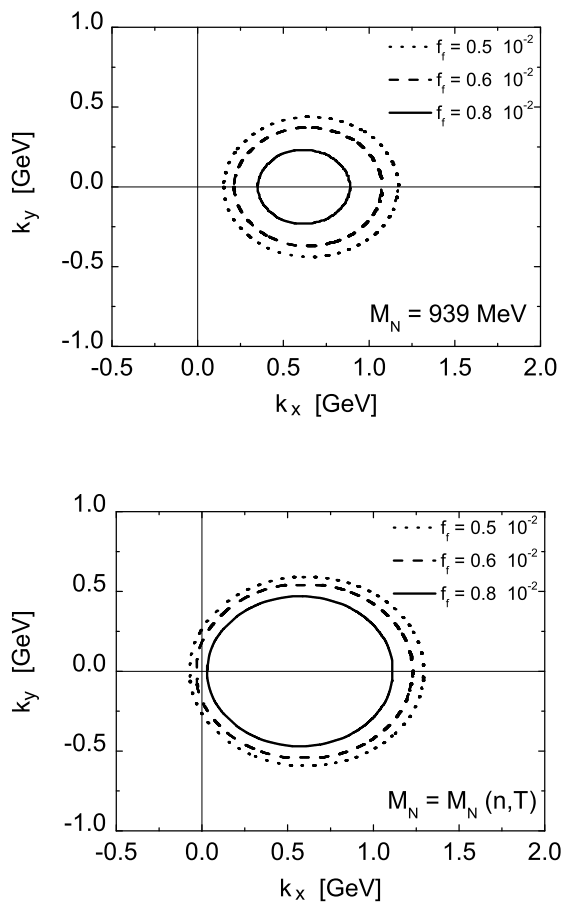


FIG. 5: Freeze out distribution functions $f_f(k_x, k_y)$ over their transversal and longitudinal momenta k_x and k_y , respectively, at $t = 9.0\tau$ in RFF. **LEFT:** Evaluation with a vacuum nucleon mass $M_N(0) = 939$ MeV. **RIGHT:** Evaluation with the density and temperature dependent nucleon mass $M_N(n, T)$. The overall norm of the Freeze out distribution function has increased by a factor of $\simeq 4$ when density and temperature dependent nucleon masses were taken into account.

three-fluid model, which is a highly involved tool, cf. [65]. Therefore, for the time being it is difficult to say how strong the impact of mesons is. Therefore, we were aiming at a description, which allows to account for the nucleon mass shift scenario during the freeze out process in a more common way.

Finally, we remark that in-medium modifications have actually to be taken into account already before and during the hadronization process. This points to an even stronger impact of in-medium modifications on the final particle spectrum than presented.

V. SUMMARY

We have investigated a freeze out scenario within a finite layer for a massive nucleon gas. Special attention has been drawn about how strong the impact of the in-medium nucleon mass modification on the thermal freeze out process is. By focussing on a purely nucleon gas we have found a substantial effect on the thermodynamical quantities like temperature T , flow velocity v , particle density n and energy density e of the interacting component. All of these thermodynamical functions have revealed a faster freeze out compared to a scenario without in-medium nucleon mass shift. These modifications have a sizable implication on the freeze out particle distribution function, which is a basic observable in heavy-ion collision experiments. For small momenta around the nucleon mass a strong change of about a factor $\simeq 2$ has been found (see Fig. 4). A contour plot of the particle distribution function in the transversal-longitudinal momentum plane (k_x, k_y) illustrates this effect (see Fig. 5). From these results we conclude that in-medium modifications of nucleons have a significant consequence on the freeze out process. This reasoning is certainly valid for heavy-ion collisions, which produce sufficiently high nucleon particle densities; in particular for experiments like Compressed Baryonic Matter (CBM collaboration) planned at the GSI facility in Darmstadt/Germany.

For a more realistic description of heavy ion collisions one should include in the analysis at least the low laying mesons and baryons as well. All hadrons suffer in-medium modifications of their masses and widths, but there are strong differences among them. For instance, while the pion mass remains almost unaffected by the hadronic medium even at very high temperatures and densities, this is not the case for nucleons, kaons and Delta resonances. Taking into account the pions and the in-medium modifications of other hadrons in the fireball produced in nucleus-nucleus reactions could modify our results in the details, but not the general statement that in-medium modifications have some relevance for the freeze out process. For example, the implementation of the pions leads to a stronger temperature dependence of the chiral condensate [53], which causes a stronger down shift of the nucleon mass with increasing temperature. Then, our results might even be more pronounced. In addition, the implementation of in-medium modifications has to be taken into account before and during the hadronization, which leads also to an amplification of their impact on the whole freeze out process.

In summary, our findings for a purely nucleon gas suggest that taking into account in-medium modifications of nucleons seems to be a necessary

and interesting phenomenon, in particular for collision scenarios with high baryonic densities.

Acknowledgements

The authors would like to express their gratitude to Prof. Jean Cleymans for enlightening discussions. S.Z. thanks for the warm hospitality at the Bergen Center for Computational Science (BCCS) and Bergen Physics Laboratory (BCPL) at the University of Bergen/Norway. S.Z. and J.M. wishes to acknowledge the NordForsk for the partial financial support of this work.

Appendix

The function G_n^\pm ($n = 1, 2$) are defined as

$$G_n^\pm(M_N, v, T) = \frac{1}{T^{n+2}} \int_0^\infty dk k \left(\sqrt{k^2 + M_N^2} \right)^n \times E_1 \left(\frac{\gamma}{T} \sqrt{k^2 + M_N^2} \pm \frac{\gamma v k}{T} \right), \quad (36)$$

where E_1 is a special case of incomplete Gamma-function [66] and defined as

$$E_1(x) = \int_x^\infty dt t^{-1} e^{-t}. \quad (37)$$

The function K_n is the Bessel function of second kind [66], defined as

$$K_n(z) = \frac{2^n n!}{(2n)!} z^{-n} \int_x^\infty dx e^{-x} (x^2 - z^2)^{n-1/2}. \quad (38)$$

Finally, we prove the vanishing of the second term in Eq. (7). First, we note explicitly the relevant four-current and energy-momentum tensor components as deduced directly from the microscopic kinetic definitions (2) and (3), respectively. We recall that due to the immediate re-thermalization

limit during the freeze out there is actually a Jüttner type distribution for f_i , but with the thermodynamical functions T and v as evaluated with the approach presented and given in Figs. 2. Therefore, at the beginning of the time-step for f_i one has to insert the Jüttner distribution (15), but with the evaluated functions T , and v , into the microscopic definitions (2) and (3), getting the following components in RFF:

$$N^0 = \frac{n}{4} [2a b K_0(a) + 4b K_1(a)], \quad (39)$$

$$\begin{aligned} N^x &= \frac{n}{4} [2v a b K_0(a) + 4v b K_1(a)], \\ T^{00} &= \frac{nT}{4} [2a b^2 K_1(a) + 2b^2 (3 + v^2) K_2(a)], \end{aligned} \quad (40) \quad (41)$$

$$\begin{aligned} T^{0x} &= -\frac{T}{\gamma v} N^0 \\ &+ \frac{nT}{4} \left[2a b^2 v K_1(a) + 2\frac{b^2}{v} (1 + 3v^2) K_2(a) \right], \end{aligned} \quad (42)$$

$$\begin{aligned} T^{xx} &= -2\frac{T}{\gamma v} N^x \\ &+ \frac{nT}{4} \left[2a b^2 v^2 K_1(a) + 2b^2 (3 + v^2) K_2(a) \right]. \end{aligned} \quad (43)$$

We recall that $a = M/T$, and $b = \gamma a$ with $\gamma = (1 - v^2)^{-1/2}$. The second term in Eq. (7) is given as

$$\begin{aligned} du_\mu T^{\mu\nu} u_\nu &= du_0 T^{00} u_0 + du_0 T^{0x} u_x \\ &+ du_x T^{x0} u_0 + du_x T^{xx} u_x. \end{aligned} \quad (44)$$

With $u_\mu = \gamma(1, -v, 0, 0)$ we get $du_0 = \gamma^3 v dv$ and $du_x = -\gamma^3 dv$. By using these relations and inserting the components (39) - (43) into (44) we immediately find $du_\mu T^{\mu\nu} u_\nu = 0$. We recall that $a K_2(a) = a K_0(a) + 2 K_1(a)$.

-
- [1] E. Shuryak, Phys. Rev. Lett. **68** 3270 (1992).
[2] T.S. Biró, E. van Doorn, B. Müller, M.H. Thoma, X.-N. Wang Phys. Rev. C **48** 1275 (1993).
[3] X.N. Wang, Nucl. Phys. A **590** 47c (1995).
[4] K. Geiger, J.I. Kapusta, Phys. Rev. D **47** 4905 (1993).
[5] P. Koch, B. Müller and J. Rafelski, Phys. Rep. **142** 167 (1986).
[6] K. Geiger, Phys. Rep. **258** 237 (1995).
[7] J. Cleymans, K. Redlich, Phys. Rev. C **60** 054908 (1999).
[8] F. Becattini, M. Gaździcki, A. Keränen, J. Manninen, R. Stock, Phys. Rev. C **69** 024905 (2004).
[9] F. Becattini, J. Cleymans, A. Keränen, E. Suohonen, K. Redlich, Phys. Rev. C **64** 024901 (2001).
[10] F. Becattini, M. Gaździcki, J. Sollfrank, Eur. Phys. J. C **5** 143 (1998).
[11] J. Cleymans, H. Satz, Z. Phys. C **57** 135 (1993).
[12] P. Braun-Munzinger, D. Magestro, K. Redlich, J. Stachel, Phys. Lett. B **518** 41 (2001).

- [13] P. Braun-Munzinger, I. Heppe, J. Stachel, Phys. Lett. B **465** 15 (1999).
- [14] J. Letessier, J. Rafelski, nucl-th/0504028 (2005); W. Florkowski, W. Broniowski, M. Michalec, Acta Phys. Pol. B **33** 761 (2002); G.D. Yen, M.I. Gorenstein, Phys. Rev. C **59** 2788 (1999); J. Sollfrank, M. Ga  dzicki, U.W. Heinz, J. Rafelski, Z. Phys. C **61** 659 (1994).
- [15] S.A. Bass, Nucl. Phys. A **698** 164 (2002).
- [16] X.-N. Wang, Nucl. Phys. A **698** 296 (2002).
- [17] P. Huovinen, Acta Phys. Pol. B **33** 1635 (2002).
- [18] W. Florkowski, W. Broniowski, Phys. Lett. B **477** 73 (2000).
- [19] D. Zschiesche, S. Schramm, J. Schaffner-Bielich, H. Stoecker, W. Greiner, Phys. Lett. B **547** 7 (2002).
- [20] T. Yamazaki et. al., Phys. Lett. B **418** 246 (1998).
- [21] V. Thorsson, A. Wirzba, Nucl. Phys. A **589** 633 (1995).
- [22] V.L. Eletsky, B.L. Ioffe, Phys. Rev. Lett. **78** 1010 (1997).
- [23] S. Mallik, S. Sarkar, Phys. Rev. C **69** 015204 (2004).
- [24] F. Laue et al. (for the KaoS collaboration), Eur. Phys. J. A **79** 397 (2000); Phys. Rev. Lett. **82** 1640 (1999).
- [25] R. Barth et al. (for the KaoS collaboration), Phys. Rev. Lett. **78** 4007 (1997).
- [26] C.L. Korpa, M.F.M. Lutz, Acta Phys. Hung. A **22** 21 (2005).
- [27] I. Tanihata, S. Nagamiya, S. Schnetzer, H. Steiner, Phys. Lett. B **100** 121 (1981).
- [28] H.W. Barz, L.P. Csernai, W. Greiner, Phys. Rev. **26** 740 (1982).
- [29] Cs. Anderlik, Z.I. L  z  r, V.K. Magas, L.P. Csernai, H. St  cker, W. Greiner, Phys. Rev. C **59** 388 (1999).
- [30] V.K. Magas, Cs. Anderlik, L.P. Csernai, F. Grassi, W. Greiner, Y. Hama, T. Kodama, Zs. L  z  r, H. St  cker, Phys. Lett. B **459** 33 (1999).
- [31] C. Anderlik, L. P. Csernai, F. Grassi, et al., Phys. Rev. C **59** 3309 (1999).
- [32] V.K. Magas, C. Anderlik, L.P. Csernai et al., Heavy Ion Phys. **9** 193 (1999).
- [33] V.K. Magas, A. Anderlik, Cs. Anderlik, L.P. Csernai, Eur. Phys. J. C **30** 255 (2003).
- [34] E. Moln  r, L.P. Csernai, V.K. Magas, A. Nyiri, K. Tam  siunas, arXiv: nucl-th/0503047.
- [35] E. Moln  r, L.P. Csernai, V.K. Magas, Zs.I. L  z  r, A. Nyiri, K. Tam  siunas, arXiv: nucl-th/0503048.
- [36] L.P. Csernai, "Introduction to Relativistic Heavy Ion Collisions", John Wiley & Sons, Chichester (1994) ISBN 0 471 93420 8.
- [37] J. Kapusta, Phys. Rev. C **29** 1735 (1984).
- [38] C. Grant, J. Kapusta, Phys. Rev. C **32** 663 (1985).
- [39] T.S. Olson, W.A. Hiscock, Phys. Rev. C **39** 1818 (1989).
- [40] F. J  ttner, Ann. Phys. und Chem. **34** 856 (1911).
- [41] C. Rebbi, "Lattice Gauge Theories and Monte Carlo Simulations", Addison Wesley, Reading, MA, (1988).
- [42] M.A. Shifman, A.I. Vainshtein, V.I. Zakharov, Nucl. Phys. B **147** 385 (1979); ibid 448; ibid 519.
- [43] B.L. Ioffe, Nucl. Phys. B **188** 317 (1981).
- [44] E.G. Drukarev, Prog. Part. Nucl. Phys. **50** 659 (2003).
- [45] R.J. Furnstahl, D.K. Griegel, T.D. Cohen, Phys. Rev. C **46** 1507 (1992).
- [46] T.D. Cohen, R.J. Furnstahl, D.K. Griegel, Prog. Part. Nucl. Phys. **35** 221 (1995).
- [47] L.S. Celenza, C.M. Shakin, "Relativistic Nuclear Physics: Theories of Structures and Scattering", World Scientific, Singapore, (1986).
- [48] J.D. Walecka, Ann. Phys. **83** 491 (1974).
- [49] A.M. Rakhimov, M.M. Musakhanov, F.C. Khanna, U.T. Yakhshiev, Phys. Rev. C **58** 1738 (1998).
- [50] R.J. Furnstahl, C.E. Price, G.E. Walker, Phys. Rev. C **36** 2590 (1987).
- [51] M. Jaminon, C. Mahaux, Phys. Rev. C **40** 354 (1989).
- [52] M. Lutz, S. Klimt, W. Weise, Nucl. Phys. A **542** 521 (1992).
- [53] S. Zschocke, B. K  mpfer, O.P. Pavlenko, Gy. Wolf, XL International Winter Meeting on Nuclear Physics, Bormio (Italy), January 20 - 26, 2002, arXiv: nucl-th/0202066.
- [54] X. Jin, T.D. Cohen, R.J. Furnstahl, D.K. Griegel, Phys. Rev. C **47** 2882 (1993).
- [55] T.D. Cohen, R.J. Furnstahl, D.K. Griegel, Phys. Rev. C **45** 1881 (1992).
- [56] S. Eidelman et al. (Particle Data Group), Phys. Lett. B **592** 1 (2004) (URL: <http://pdg.lbl.gov>).
- [57] When a numerical value for the chiral condensate is fixed, then the current quark mass $m_q = (m_u + m_d)/2$ is determined by the Gell-Mann–Oakes–Renner relation: $m_\pi^2 f_\pi^2 = -2m_q \langle 0|\bar{q}q|0 \rangle$; $f_\pi = 92$ MeV is the pion decay constant and $m_\pi = 138$ MeV is the pion mass.
- [58] C. Runge, Math. Ann. **46** 167 (1895).
- [59] M.W. Kutta, Z. f. Math. u. Phys. **46** 435 (1901).
- [60] J.D. Lambert, D. Lambert, "Numerical Methods for Ordinary Differential Systems: The Initial Value Problem", New York, Wiley (1991).
- [61] P. Braun-Munzinger, J. Stachel, J.P. Wessels, N. Xu, Phys. Lett. B **344** 43 (1995).
- [62] J. Cleymans, H. Oeschler, K. Redlich, Phys. Rev. C **59** 1663 (1999).
- [63] At point A of the freeze out front the corresponding values are $d\sigma_\mu^{\text{RFF}} = (1, 0, 0, 0)$, $k_\mu^{\text{RFF}} = (E_k, |\mathbf{k}| \cos\Theta_k, 0, 0)$, where Θ_k is the angle between the Freeze out normal three vector $d\sigma$ and the three-momentum \mathbf{k} of the particle.
- [64] E.L. Bratkovskaya, W. Cassing, C. Greiner, M. Effenberger, U. Mosel, A. Sibirtsev, Nucl. Phys. A **681** 84 (2001).
- [65] L. P. Csernai, I. Lovas, J.A. Maruhn, A. Rosenhauer, J. Zim  nyi, W. Greiner, Phys. Rev. C **26** 149 (1982).
- [66] M. Abramowitz, I.A. Stegun, "Handbook of Mathematical Functions", Dover Publ. Inc., New York, 1970, ISBN 0 486 61272 4.